Journal of Thermal Analysis and Calorimetry, Vol. 75 (2004) 63–71

PHASE EQUILIBRIA IN THE Ag_4SSe–SnTe SYSTEM

V. Vassilev[*], *L. Aljihmani and V. Parvanova*

University of Chemical Technology and Metallurgy, 8 Kliment Ohridski blvd., 1756 Sofia, Bulgaria

(Received July 9, 2003; in revised form September 31, 2003)

Abstract

The phase diagram of the system Ag_4SSe–SnTe is studied by means of X-ray diffraction, differential thermal and metallographic analyses and measurements of the microhardness and the density of the material. This diagram is divided into two eutectic-type subdiagrams by the composition $Ag_4SSe\cdot 2SnTe$. The unit-cell parameters of the intermediate phases $3Ag_4SSe\cdot SnTe$ (phase A) and α-$Ag_4SSe\cdot 2SnTe$ (phase B) are determined as follows: for phase A: a=0.7851 nm, b=0.7196 nm, c=0.6296 nm, α=101.32°, β=85.90°, γ=111.36°; for phase B: a=0.3662 nm, b=0.3303 nm, c=0.3343 nm, α=90.74°, β=108.94°, γ=91.91°. The phase $Ag_4SSe\cdot 2SnTe$ melts congruently at 615°C and a polymorphic transition of the phase takes place at $T_{\alpha\leftrightarrow\beta}$=110°C.

Keywords: Ag_4SSe–SnTe, differential thermal analysis, phase diagram, X-ray diffraction

Introduction

The combination of the compounds Ag_4SSe and SnTe has not been studied in relation with the phase equilibria. Investigation of such a binary system is of a definite scientific and practical interest because components with different properties are involved. The composition AgSSe exists in the nature and is known as the mineral Aguilarite [1, 2]. It is synthesised for first time by Earley by means of a direct synthesis [3]. Its existence is confirmed also at investigation of the phase diagram of the system Ag_2S–Ag_2Se [4]. The phase transition α-Ag_4SSe→β-Ag_4SSe takes place at 100±5°C and the compound melts at 815°C [4]. The thermal energy gap of Ag_4SSe is 0.24±0.01 eV [5]. The conductivity of the material and its electron mobility and concentration at 300 K are 500 S cm^{-1}, 350 cm^2 V^{-1} s^{-1} and $6.5\cdot 10^{18}$ cm^{-3}, respectively [5]. Ag_4SSe exhibits good thermoelectric properties [5, 6].

SnTe is the only compound within the system Sn–Te that melts congruently at 790°C [7, 8]. The maximum melting temperature (805.9±0.3°C) corresponds to an alloy containing 50.8 mol% Te [9]. SnTe has a NaCl-type structure (with a=0.63 nm and coordination number z=4) [11]. SnTe is a semimetal with energy gap ΔE=0.18 eV [10] and conductivity 8000–9000 S cm^{-1} in the temperature range 140–800 K [12, 13]. At

---

[*] Author for correspondence: E-mail: venciv@uctm.edu

1388–6150/2004/ $ 20.00

Akadémiai Kiadó, Budapest
Kluwer Academic Publishers, Dordrecht

normal conditions SnTe is always a *p*-type semiconductor with high hole concentration. This concentration is increased with increasing the Te content and varies from $2\cdot10^{20}$ up to $1.5\cdot10^{21}$ cm^{-1} [12]. The maximum mobility measured at 300 K is $\mu_p=1\cdot10^3$ cm^2 V^{-1} s^{-1} [10]. Monocrystal and polycrystal layers of SnTe [14, 15] are used for fabrication of epitaxial heterostructures $Pb_{1-x}Sn_xTe$ [16, 17], SnTe–Cd(S, Se) [14] and others on substrates of PbTe, Si, $A^{II}B^{IV}$, $A^{III}B^{V}$ and others.

The main goal of this work is the investigation of the phase equilibria in the system Ag_4SSe–SnTe by the means of the conventional differential thermal analysis (DTA) [18– 21], and X-ray powder diffraction (XRD) [18, 19] as well as determining the limits of the solid solutions and the compositions of the intermediate phases (if such exist), thus building a base for a further complex investigation.

Experimental

The system $(Ag_4SSe)_{100-x}(SnTe)_x$ was studied over 21 compositions within the concentration range 0–100 mol% SnTe. The compositions were prepared through a direct mono-temperature synthesis [10] mixing in proper ratio Ag_4SSe and SnTe in evacuated and sealed quartz ampoules. Ag_4SSe and SnTe were obtained by the same method from initial elements with purity 4N (Ag, Sn, S) and 5N (Se, Te). For the synthesis of the compositions rich of SnTe the internal surface of the ampoules was preliminary covered with graphite. The maximum temperature and the duration of the synthesis were 1050°C and 1 h, respectively. A vibrational stirring of the melt was applied. As a final step the melts were homogenized at 600°C for 3 h.

The phase transformations in the samples were investigated by means of several methods as follows: DTA (equipment of the system Paulik– Paulik–Erdey made by MOM, Hungary) at heating rate of 10°C min^{-1}; reference substance (calcinated γ-Al_2O_3) and the studied substain weighed 0.3 g and was placed in evacuated and sealed quartz ampoules at pressure equal to 0.1 Pa; XRD (equipment TUR-M61) with CuK_α irradiation and Ni-filter, $\theta=5$–40°; microstructure analysis (microscope MIM-7). Measurements of the microhardness (instrument PMT-3 at loading 10 and 20 g) and of the density of the material (hydrostatic technique with toluene as reference liquid) were carried out as well.

Results and discussion

The data obtained from the X-ray diffraction analyses are summarized in a schematic diagram (Fig. 1). They are in a complete agreement with the results reported previously in the literature [1, 23].

Within the range of concentrations 0–100 mol% SnTe new lines are observed, different from those of Ag_4SSe and SnTe. They are of maximum intensity and best pronounced for compositions containing 25.0 and 66.7 mol% SnTe, respectively. These data suggest the existence of two intermediate phases with compositions $3Ag_4SSe\cdot SnTe$ (phase A) and α-$Ag_4SSe\cdot 2SnTe$ (phase B) [18].

Table 1 Data from indexing of phase $3Ag_4SSe \cdot SnTe$

No.	d_{exp}/Å	$100I/I_0$/%	$Q=1/d^2$	hkl	$d_{calc.}$/Å
1	7.29	5	0.0188	100	7.312
2	6.65	6	0.0226	010	6.588
3	6.23	14	0.0258	001	6.174
4	3.83	7	0.0682	$2\bar{1}0$	3.830
5	3.30	29	0.0918	020	3.294
6	3.159	100	0.1002	$02\bar{1}$	3.156
7	2.846	5	0.1235	102, $\bar{1}02$	2.844
8	2.80	6	0.1276	210	2.800
9	2.71	15	0.1362	021	2.707
10	2.58	6	0.1502	$1\bar{2}2$, $\bar{1}12$	2.582
11	2.51	16	0.1587	$02\bar{2}$	2.492
12	2.43	6	0.1694	300	2.437
13	2.35	9	0.1811	202	2.359
14	2.23	31	0.2011	030, $0\bar{3}1$	2.200
15	2.10	40	0.2268	220	2.101
16	2.06	5	0.2356	003	2.058
17	1.93	40	0.2685	$13\bar{1}$, $\bar{3}12$	1.925
18	1.85	19	0.2922	$\bar{1}13$	1.857
19	1.73	9	0.3341	$1\bar{3}3$	1.724
20	1.67	6	0.3586	321, $04\bar{1}$	1.669
21	1.65	11	0.3673	040	1.647
22	1.60	5	0.3906	213	1.600
23	1.58	4	0.4006	$\bar{3}22$	1.578
24	1.53	5	0.4270	123	1.524
25	1.45	6	0.4756	500	1.462
26	1.43	6	0.4890	322	1.428
27	1.41	7	0.5030	$3\bar{5}1$	1.411

The unit-cell parameters of the phases $3Ag_4SSe \cdot SnTe$ (phase A) and α-$Ag_4SSe \cdot 2SnTe$ (phase B) previously kept at the temperature 90±5°C for 720 h and frozen in a mixture of H_2O+ice are determined by the Ito's method [24] as follows: for phase A: $a=0.7851$ nm, $b=0.7196$ nm, $c=0.6296$ nm, $\alpha=101.32°$, $\beta=85.90°$, $\gamma=111.36°$; for phase B: $a=0.3662$ nm, $b=0.3303$ nm, $c=0.3343$ nm, $\alpha=90.74°$, $\beta=108.94°$, $\gamma=91.91°$. The indexing data of these phases are given in Tables 1 and 2, respectively.

Table 2 Data from indexing of low-temperature phase, α-$Ag_4SSe \cdot 2SnTe$

No.	d_{exp}/Å	$100I/I_0$/%	$Q=1/d^2$	*hkl*	$d_{calc.}$/Å
1	3.46	10	0.0835	100	3.461
2	3.30	5	0.0918	010	3.300
3	3.16	6	0.1001	001	3.161
4	2.84	100	0.1240	$10\bar{1}$	2.839
5	2.44	3	0.1680	$1\bar{1}1$	2.431
6	2.34	15	0.1826	110	2.342
7	2.30	23	0.1890	$01\bar{1}$	2.312
8	2.174	13	0.2116	$\bar{1}11$	2.163
9	2.15	11	0.2163	$11\bar{1}$	2.141
10	2.028	29	0.2431	101	2.029
11	1.80	6	0.3016	$20\bar{1}$	1.781
12	1.78	9	0.3086	$1\bar{1}1$	1.759
13	1.73	12	0.3341	200	1.731
14	1.71	5	0.3420	111	1.699
15	1.65	3	0.3673	020	1.650
16	1.44	5	0.4823	$01\bar{2}$	1.44
17	1.41	14	0.5021	012	1.412
18	1.39	9	0.5176	201	1.345
19	1.29	7	0.6009	102	1.288
20	1.28	6	0.6104	$2\bar{1}1$	1.264

From the heating curves and the observed endoeffects of the curves the maximum temperatures of the different phase transformations were determined. They are given in Table 3.

The endothermal effects from the second up to sixth columns are of small area but well pronounced. Outstanding are the effects for compositions containing 40 and 75 mol% SnTe at 525 and 550°C, respectively. These peaks are of considerably greater area and probably they correspond to some non-variant points. The thermoeffects from each column (columns 2 to 6) are obtained at equal temperatures. Thus they have to be related to different non-variant equilibria. The high-temperature effects corresponding to the liquidus line (column 7) are better pronounced and of greater area compared with the effects corresponding to the non-variant equilibria (columns 2 to 6).

The microstructure of the samples containing 40 to 60 mol% SnTe was developed by an etching solution $HNO_3:HF:H_2O:CH_3COOH:Br_2=10:10:5:1:0.2$ ($\tau=1–10$ s, $t=70$°C), and that of the samples containing 10 to 25 mol% SnTe – by etching solution $HNO_3:H_2O=1:4$ ($\tau=60–120$ s; $t=40$°C). The microstructure of the other samples of the system investigated was developed at the step ‘polishing’ with Cr_2O_3. Samples contain-

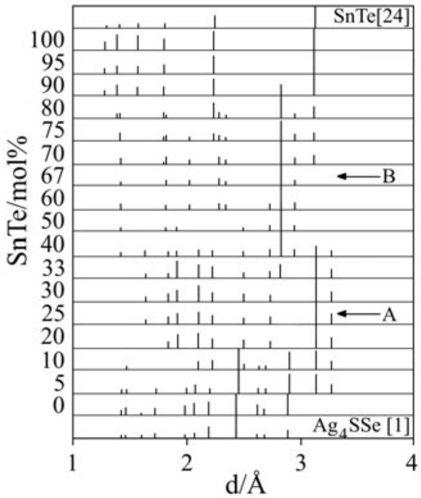

Fig. 1 Schematic diagram of the X-ray diffraction lines for the system Ag_4SSe–SnTe

ing 25 and 66.7 mol% SnTe, as well as the starting components Ag_4SSe and SnTe are mono-phasic and all others-two-phasic.

Table 3 Temperatures of endothermal effects recorded on DTA curves of investigated samples

SnTe/mol%	Temperature of endothermal effects/°C						
0	105	–	–	–	–	–	820
5	75	65	–	–	535	–	795
10	–	65	–	–	535	–	790
20	–	70	–	–	540	–	775
25	–	–	–	–	535	–	750
30	–	–	–	520	540	–	735
33.3	–	–	–	525	–	–	725
40	–	–	100	525	–	–	525
50	–	–	100	520	–	–	580
60	–	–	105	525	–	–	600
66.7	–	–	110	–	–	–	615
70	–	–	115	–	–	550	605
75	–	–	115	–	–	550	550
80	–	–	110	–	–	555	570
90	–	–	105	–	–	550	635
95	–	–	115	–	535	–	705
100	–	–	–	–	–	–	810

For the concentration ranges 0–25.0; 25.0–66.7 and 66.7–100.0 mol% SnTe two values of the microhardness (HV) are obtained for each of them. Two of these values have to be related to the starting components, Ag_4SSe and SnTe, respectively, and other two-to the intermediate phases $3Ag_4SSe·SnTe$ and $Ag_4SSe·2SnTe$ Fig. 2. The microhardness of the phases $Ag_4SSe·SnTe$ and $Ag_4SSe·2SnTe$ is 40–42 and 59–61 kgf mm^{-2}, and that of the starting components Ag_4SSe and SnTe–21 kgf mm^{-2} [4] and 70 kgf mm^{-2} [25], respectively.

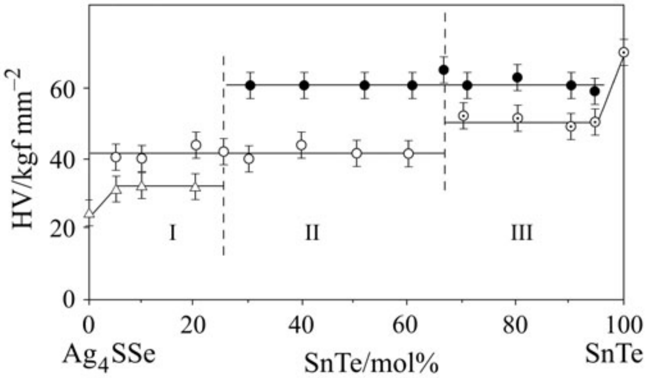

Fig. 2 Dependence HV(x) for samples of the system Ag_4SSe–SnTe

The density (d) of the samples from the Ag_4SSe–SnTe system varies in the limits 6.4–7.4 g cm^{-3} Fig. 3. Within the concentration limits 0–100 mol% SnTe the additive law is not followed suggesting that complex physico-chemical processes take place. Probably, the intermediate phases $3Ag_4SSe·SnTe$ and $Ag_4SSe·2SnTe$ are obtained as a result of these processes.

In the concentration limits 0–5 mol% SnTe a shift of the lines is observed, that is an indication for the existence of a limited area of solid solutions based on Ag_4SSe (Fig. 1). The intermediate phases A and B are stoichiometric.

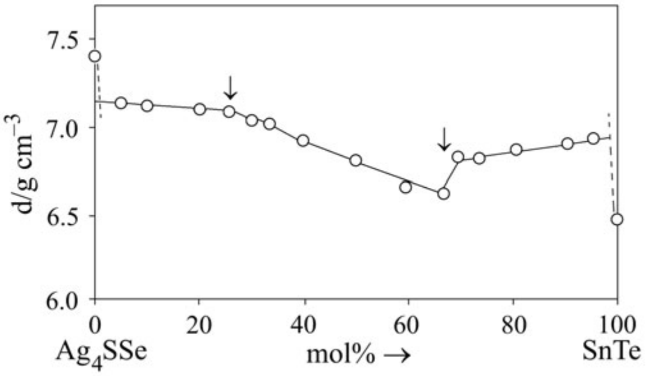

Fig. 3 Dependence $d(x)$ for samples of the system Ag_4SSe–SnTe

Within the limits 5–25, 25.0–66.7 and 66.7–100.0 mol% SnTe lines of two phases are observed simultaneously: phase Ag_4SSe+A; A+B and phase B+SnTe i.e. these concentration ranges correspond to two-phasic fields in the phase diagram of the system Ag_4SSe–SnTe.

The gradual variation of the dependence HV(x) in the ranges $0<x<5$ and $95<x<100$ mol% SnTe suggests the presence of boundary solid solutions based on Ag_4SSe and SnTe (Fig. 2).

The observed specific variation of the dependence $d(x)$ at x=25 and x=66.7 mol% SnTe is related to the existence of the intermediate phases $3Ag_4SSe\cdot SnTe$ and $Ag_4SSe\cdot 2SnTe$ (Fig. 3). The abrupt variation of d in the ranges 0–5 and 95–100 mol% is connected with the presence of solid solutions based on Ag_4SSe and SnTe (Fig. 3).

On the basis of the data from the DTA, the X-ray diffraction analysis, investigation of the microstructure and measurements of the microhardness and the density the phase diagram of the system Ag_4SSe–SnTe (Fig. 4) is built-up. This phase diagram has a complex structure characterised with the following peculiarities:

1) There are four non-variant equilibria: two eutectic at x=75 and 40 mol% SnTe and t=550 and 530°C, respectively; one peritectic with coordinates of the peritectic point $x\cong75$ mol% and t=540°C and one eutectoidal equilibrium with coordinates of the eutectoidal point x=10 mol% SnTe and t=70°C.

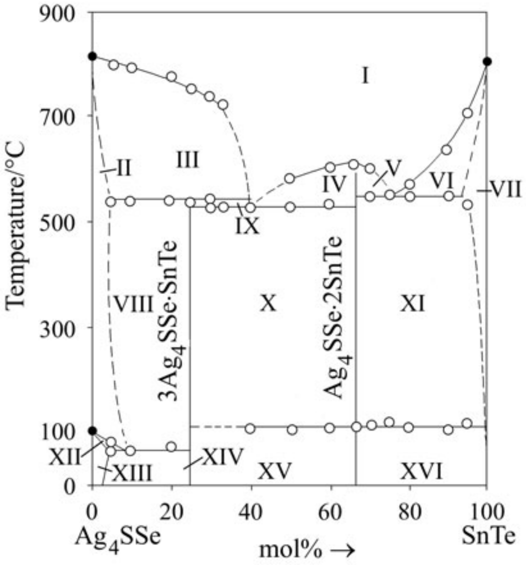

Fig. 4 Phase diagram of the system Ag_4SSe–SnTe. I–Liquid (melt-L); II–β-Ag_4SSe (solid solution based on Ag_4SSe); III–β-Ag_4SSe+L; IV–L+β-$Ag_4SSe\cdot 2SnTe$; V–β-$Ag_4SSe\cdot 2SnTe$+L; VI–L+α-SnTe; VII–α-SnTe (solid solution based on SnTe); VIII–β-Ag_4SSe+$3Ag_4SSe\cdot SnTe$; IX-$3Ag_4SSe\cdot SnTe$+L; X–$3Ag_4SSe\cdot SnTe$+β-$Ag_4SSe\cdot 2SnTe$; XI–β-$Ag_4SSe\cdot 2SnTe$+α-SnTe; XII–α-Ag_4SSe+β-Ag_4SSe; XIII–α-Ag_4SSe (solid solution based on α-Ag_4SSe); XIV–α-Ag_4SSe+$3Ag_4SSe\cdot SnTe$; XV–$3Ag_4SSe\cdot SnTe$+α-$Ag_4SSe\cdot 2SnTe$; XVI–α-$Ag_4SSe\cdot 2SnTe$+α-SnTe

2) As a result of various physico–chemical interactions taking place two intermediate phases with most probable compositions $3Ag_4SSe \cdot SnTe$ (phase A) and $Ag_4SSe \cdot 2SnTe$ (phase B). Phase A exists within the temperature range 20–540°C. It melts incongruently, i.e. the peritectic reaction

$$\beta\text{-}Ag_4SSe+L \xleftrightarrow{540\pm10°C} 3Ag_4SSe \cdot SnTe$$

takes place.

The intermediate phase B undergoes a polymorphic transition at $T_{\alpha\leftrightarrow\beta}=110\pm10°C$ proved by the help of DTA and XRD methods described by Arai *et al.* [22] and Moriya *et al.* [26].

It melts congruently at 615±10°C but tends to dissociate (has a rounded liquidus line). The intermediate phase B divides the phase diagram into two eutectic-type subdiagrams Ag_4SSe–B and B–SnTe.

3) There are regions of boundary solid solutions based on Ag_4SSe and SnTe. The solid solutions based on α-Ag_4SSe turn into solid solutions based on β-Ag_4SSe through the two-phase region XII of the phase diagram. The temperature of the transition $\alpha\leftrightarrow\beta$ depends on the composition and varies from 70 to 105°C. The regions of homogeneity based on α-Ag_4SSe and β-Ag_4SSe expand at increasing the temperature and have maximum values at x=5 mol% SnTe and t=70°C and at x=93 mol% SnTe and t=550°C. A shift of the SnTe-lines is not observed at room temperature i.e. SnTe does not dissolve Ag_4SSe.

Conclusions

By means of five independent technics the phase diagram of the system Ag_4SSe–SnTe is built-up. As a result of complex physico–chemical processes in solid- and liquid-state two intermediate phases are formed with most probable compositions $3Ag_4SSe \cdot SnTe$ (phase A) and $Ag_4SSe \cdot 2SnTe$ (phase B). These two phases together with the starting components and the polymorphism of Ag_4SSe and phase B cause the existence of 15 phasic fields. Four of the fields are mono-phasic and the rest of them two-phasic. Of particular interest is the solid solution based on the low-temperature modification α-Ag_4SSe that possesses semiconductor properties.

* * *

The authors acknowledge thankfully the financial support for this work from the Ministry of Education and Science (Fond ‘Scientific investigations’-contract TN-1102).

References

1 American Society of Testing Materials, Philadelphia 1969, ASTM 6-0550.
2 American Society of Testing Materials, Philadelphia 1969, ASTM 27-620.
3 J. W. Earley, Amer. Mineralogist, 35 (1950) 337.
4 Z. Boncheva-Mladenova and K. Zaneva, J. Anorg. Allg. Chem., 437 (1977) 253.
5 V. Vasilev and Z. Boncheva-Mladenova, Annual VCTI 27, 1 (1984) 143 (in Bulgarian).

6 V. Vasilev, Z. Boncheva-Mladenova and K. Kirova, Annual VCTI, 28, 1 (1981) 136 (in Bulgarian).
7 M. Hansen and K. Anderko, Struktura Dvoiniih Splavov, Metallurgizdat, Moscow 1962, p. 1488 (in Russian).
8 N. H. Abrikosov and L. E. Shelimova, Poluprovodnikovie Materiali na Osnove Soedineniya $A^{II}B^{IV}$, Nauka, Moscow 1975, p. 195 (in Russian).
9 V. M. Glazov, L. M. Pavlova and A. V. Shcheshin, J. Neorganicheskoi. Himii, 33 (1988) 2388 (in Russian).
10 Z. Boncheva-Mladenova and V. S. Vassilev, Himia I Fizikohimia na poluprovodnikovite materiali, Narodna Prosveta, Sofia 1991, p. 298 (in Bulgarian).
11 D. M. Chizikov and B. P. Schastlivii, Tellur i Telluridii, Nauka, Moskow 1966, p. 200 (in Russian).
12 P. Fielding and G. Fisher, Phys. Chem. Solids, 8 (1959) 434.
13 P. Bro, J. Electrochem. Soc., 109 (1962) 1110.
15 L. D. Budennaya, P. P. Gorbik, I. V. Dubrovin, V. M. Ognenko and V. V. Teterkin, Russiiskaya AN Neorg. Mater., 31 (1995) 727 (in Russian).
16 H. Y. Lee, Y. S. Kang, M. S. Jang, H. Tanaka and T. Kawai, J. Korean Phys. Soc., 37 (2000) 474.
17 O. N. Tsarenko and S. I. Ryabets, Neorgan. Mater., 4 (1999) 374 (in Russian).
18 S. Weise, V. Kramer, J. Therm. Anal. Cal., 71 (1999) 159.
19 E. Filipec, J. Therm. Anal. Cal., 56 (2003) 1035.
20 M. Hichiri, C. Favotto, H. Zamali, Y. Feutelais, B. Legendre, A. Sebaoun and M. Jemal, J. Therm. Anal. Cal., 69 (2002) 509.
21 A. Wojakowska, E. Krzyzak and A. Wojakowski, J. Therm. Anal. Cal., 65 (2001) 491.
22 M. Arai, T. Sakuma, T. Atake and N. Kawaji, J. Therm. Anal. Cal., 69 (2003) 905.
23 American Society of Testing Materials, Philadelphia 1969, ASTM 8-487.
24 T. Ito, X-ray studies on polymorphism, Maruzen Co. Ltd., Tokyo 1950, p. 187.
25 L. E. Shelimova and N. H. Abrikossov, J. Neorg. Chim., 9 (1964) 1879 (in Russian).
26 K. Moriya, T. Yamada, K. Sakai, S. Yano, S. Baluja, T. Matsuo, I. Pritz and Y. M. Vysochanskii, J. Therm. Anal. Cal., 70 (2002) 321.